Abdominal Imaging

Published online: 26 March 2014

Abdom Imaging (2014) 39:963–968
DOI: 10.1007/s00261-014-0125-x

Radiation-induced liver disease as a mimic of liver metastases at serial PET/CT during neoadjuvant chemoradiation of distal esophageal cancer

Michael J. Grant, Ryne A. Didier, Jeffrey S. Stevens, Dmitry D. Beyder, John G. Hunter, Charles R. Thomas, Fergus V. Coakley

Departments of Diagnostic Radiology (MJG, RAD, JSS, DDB, FVC), Surgery (JGH) and Radiation Oncology (CRT), Oregon Health & Science University, 3181 SW Sam Jackson Park Road, Mail Code: L340, Portland, OR 97239, USA

Abstract

Purpose: To determine the frequency and appearance of radiation-induced liver disease on PET/CT in patients undergoing serial imaging during neoadjuvant chemoradiation of distal esophageal cancer.
Materials and methods: In this IRB-approved, HIPAA–compliant retrospective analysis, we identified 112 patients with distal esophageal cancer treated by neoadjuvant chemoradiation who had serial PET/CT imaging available for review. Two readers reviewed all studies in consensus and recorded those cases where new foci of visually detectable increased FDG avidity appeared in the liver during therapy. The etiology of such foci was determined from corresponding findings at CT or MRI, by hepatic biopsy during surgery, by characteristic evolution on post-operative imaging, or by a combination of these methods.
Results: New foci of FDG avidity developed in the liver during neoadjuvant therapy in 10 of 112 (9%) patients, of whom nine (8%) were determined to have radiation-induced liver disease based on further imaging and/or biopsy and one of whom had developed interval metastatic disease based on biopsy. In the cases of radiation-induced liver disease, the abnormal foci were found only in the caudate and left hepatic lobes, near the primary tumor, while the patient who developed interval metastatic disease had involvement of the inferior right hepatic lobe, remote from the radiation therapy field.
Conclusion: New foci of increased FDG avidity are commonly seen in the caudate and left hepatic lobes of the liver during neoadjuvant chemoradiation of distal esophageal cancer, and these findings generally reflect radiation-induced liver disease rather than metastatic disease.

Key words: Radiation-induced liver disease— Esophageal cancer— PET/CT

An estimated 17990 new cases of esophageal cancer will be diagnosed in the United States during 2013, with 15210 deaths due to the disease [1]. Neoadjuvant chemoradiation, in appropriately selected patients, seems to improve survival and reduce local recurrence [2–8] and has become an increasingly common management strategy. In parallel with this therapeutic advance, PET/CT has become increasingly used as valuable imaging tools, both for baseline staging and for evaluation of treatment response [7–14]. However, it is known that radiation-induced liver disease can be a complication of radiotherapy, and one small study ($n = 26$) suggested that it may cause potentially confusing increased FDG avidity in the liver [13]. Therefore, we undertook this study to determine the frequency and appearance of radiation-induced liver disease on PET/CT in patients undergoing serial imaging during neoadjuvant chemoradiation of distal esophageal cancer.

Materials and methods

Subjects

This was a retrospective single institutional study approved by our Institutional Review Board with waiver of the requirement for informed consent. The study was

Correspondence to: Fergus V. Coakley; *email:* Coakleyf@ohsu.edu

compliant with the Health Insurance Portability and Accountability Act. We performed a search of our institutional multidisciniplary esophageal cancer conference patient database, and identified all patients ($n = 112$) between 2006 and 2013 who met the following inclusion criteria:

1. Pathologically proven distal esophageal cancer.
2. Baseline and post-neoadjuvant chemoradiation PET/CT imaging available on our institutional picture archiving and communication system (PACS—Impax; Agfa, Mortsel, Belgium). All except one patient with post-treatment PET/CT, studies were performed within 4 to 8 weeks after cessation of chemoradiation. One patient had post-treatment PET/CT 5 months after completion of therapy.
3. Documentation of radiotherapy and dose available in our electronic medical record (EPIC Hyperspace 2010). Details were recorded by the principal investigator (—).

The final study population ($n = 112$) consisted of 93 men and 19 women, with a mean age of 57 years (range 28–81). Histological diagnoses were esophageal adenocarcinoma ($n = 97$), squamous cell carcinoma ($n = 21$), and cancer not otherwise specified ($n = 4$).

Radiotherapy technique

All patients who received their radiotherapy at our institution ($n = 20$) were treated on an integrated CT and intensity modulated radiation therapy (IMRT) device (Tomotherapy TomoHD; Accuray, Madison, WI, USA). Patients initially underwent a volumetric planning CT examination to define the gross tumor volume, clinical target volume, and planning target volume. The gross tumor volume encompasses the primary tumor and clinically positive lymph nodes seen on the baseline/pretreatment radiologic examinations, including PET/CT with all lesions exhibiting an FDG avidity of maximum standard uptake values (SUV_{max}) >3. Other modalities included in determining the gross tumor volume include diagnostic and treatment planning CT, fluoroscopic studies, endoscopic ultrasound, and esophagogastroduodenoscopy. The clinical tumor volume includes the gross tumor volume plus a 0.5–1 cm radial margin as well as a 3–5 cm craniocaudal margin. The extended margins of the clinical tumor volume account for microscopic tumor extension. Also included in the clinical tumor volume is a 1.0 cm margin for any grossly involved lymph nodes and the celiac and peri-gastric nodes. The planning tumor volume adds an additional 1.0 cm to the clinical tumor volume in all directions. The volumetric planning CT was performed in either the supine or prone positions in an immobilization device, with patients in the actual treatment position. Contiguous 3-mm-thick axial CT slices through the tumor as well as any involved nodal groups were acquired. The remaining regions of disease are also scanned at 8-10 mm slice thickness extending as inferiorly as the third lumbar vertebral body in the cases of distal esophageal cancer. Intravenous iodinated contrast was only administered, if no prior contrast-enhanced CT was performed for delineation of major blood vessels. Positive enteric contrast was administered in all cases 1 hour before scanning to opacify the stomach, and oral paste was given at the time of simulation to coat the esophagus. All patients were treated with the planning tumor volume field and dosages ranged from 41.4 to 50.4 Gy in 1.8 Gy fractions. Patients treated at other facilities ($n = 92$) extended the total range of dosage from 45 Gy to 64 Gy, with 1.8 Gy fractions.

PET/CT technique

A total of 109 PET/CT scans were performed at our institution (42 baseline and 67 post-treatment studies) on an integrated PET/CT scanner (GEMINI TF, Phillips Medical Systems, Cleveland, OH, USA). Prior to scanning, patients fasted for at least 6 h with no caffeine, alcohol, or nicotine products 24 h prior to examination. All patients drank at least eight glasses of water and abstained from heavy exercise and/or muscular activity the day before the examination. Blood glucose levels were determined utilizing a point-of-care glucometer approximately 4 h before examination, and in all cases, blood glucose levels were less than 200 g/dL. Patients were injected with a mean of 12 mCi (range 10–14 mCi) of ^{18}F-radioactively-labeled FDG. After injection, the patients rested for 60 min in quiet conditions and drank 1000 mL of water 20 min before imaging time. Immediately before the PET examination, patients emptied their bladder.

Non-contrast CT scanning was then performed from the skull base through the thighs (40–90 mAs, 120 kVp, 5 mm thick slices, 5 mm increments) on the integrated multidetector device. PET images were acquired immediately following the CT scan, which were performed from the skull base to the thighs in 60–120 s per bed position depending upon the patient's weight. Reconstruction of the PET images utilized the standard vendor-provided reconstruction algorithms that employed Line-of-Response Row-Action Maximum Likelihood Algorithm (LOR-RAMLA). The CT component of the examination was utilized for attenuation correction. The PET data was corrected for dead-time losses, scatter, and random events through the manufacturer's software package.

An additional 115 PET/CT examinations (70 baseline and 45 post-treatment studies) utilized in our analysis were performed at outside/referring medical institutions

Table 1. PET findings, final diagnosis, and reference standard in the ten patients found to have foci of increased FDG avidity in the liver during neoadjuvant chemoradiation for distal esophageal cancer

Location	Lesion SUV_{max}	Diagnosis	Reference standard	Features of Radiation-induced liver disease on CT and/or MRI?[a]	Age	Sex
Left lobe	5.4	Radiation-induced liver disease	CE-CT, biopsy, and resolution on follow up CE-CT	Yes	64	Male
Caudate lobe	5.9	Radiation-induced liver disease	CE-CT, CE-MRI, resolution on follow up CE-CT and biopsy	Yes	46	Male
Inferior right lobe	12.8	Metastasis	CE-CT, persistence on follow up PET/CTs, and biopsy	No	54	Male
Left lobe	3.4	Radiation-induced liver disease	CE-CT, resolution on follow up PET/CT and CE-CT	No	66	Male
Left lobe	N/A[b]	Radiation-induced liver disease	Resolution on follow up PET/CT and CE-CT	No (did not receive same-day contrast-enhanced CT/MRI)	60	Female
Caudate lobe	N/A[b]	Radiation-induced liver disease	CE-CT, resolution on follow up CE-CT	Yes	50	Male
Caudate and left lobes	8.8	Radiation-induced liver disease	CE-CT, resolution on subsequent CE-CT	Yes	54	Female
Caudate and left lobes	6.0	Radiation-induced liver disease	CE-CT and resolution on follow up CE-CT	Yes	63	Male
Left lobe	5.0	Radiation-induced liver disease	Normal on short-term subsequent CE-MRI	No (contrast-enhanced MRI was performed 8 days later and was negative)	65	Male
Caudate lobe	5.7	Radiation-induced liver disease	CE-MRI and resolution on subsequent CE-CT	Yes	46	Male

CE-CT, Contrast-Enhanced CT; CE-MRI, Contrast-Enhanced MRI)
[a]Reported SUV measurements from outside institution reports without mention of liver background FDG avidity, precluding accurate SUV measurements
[b]Studies performed at outside institution, precluding accurate SUV measurement
[c]Please refer to "Reference Standard" section under "Materials and Methods" for discussion of characteristic imaging findings in Radiation-induced liver disease

for a total of 224. All PET/CTs except one of these were performed on integrated machines. Fasting periods, blood glucose level determination, and ^{18}F-FDG doses were performed under the general accepted guidelines of the referring medical institutions.

PET/CT image interpretation

All PET/CT images were reviewed on our institutional PACS by two board certified radiologists (—, —). By consensus, readers determined if foci of increased FDG avidity were present in the liver on baseline and post-radiation scans. A focus of increased hepatic FDG avidity was defined as a region of increased FDG uptake in the liver that was visually detectable over the normal mottled activity of the background liver. For those abnormal studies which were performed at our institution, 3D region of interest cursors was used to measure SUV_{max} within the detected abnormalities where subjectively increased FDG avidity was evident. Determination of background hepatic FDG avidity utilized a SUV_{max} mean of 5 separate random hepatic parenchymal locations measured with 3D region of interest cursors.

Reference standard

In the patients who were identified as having new foci of hepatic FDG avidity developing on post-chemoradiation PET/CT scanning, all available clinical, surgical, pathological, and radiological records were examined to establish the underlying diagnosis. Typical geographic regions of hypoattenuation with straight margins on the CT for attenuation correlation (CTAC; performed in conjunction with the PET) were considered diagnostic of radiation-induced liver disease [14–17]. Contrast-enhanced CT scan criteria for confirmation of radiation-induced liver disease included regions with well-demarcated angular/polygonal margins exhibiting arterial and portal venous hypoenhancement with delayed phase hyperenhancement that corresponded to the intrahepatic FDG-avid foci [14–19]. In patients with short interval follow up MRI, sharply delineated polygonal regions of early and persistent enhancement with low T1 and high T2 signal that mapped to the intrahepatic FDG-avid foci were used to diagnose radiation-induced liver disease [15–17, 19, 20]. Lack of mass effect on all three modalities further indicated radiation-induced liver disease [21, 22]. Resolution of the PET, CT, and MRI abnormalities on subsequent examinations also qualified as diagnostic of radiation-induced liver disease. Patients were considered to have metastatic disease, if there was interval increasing growth and/or persistent FDG avidity on subsequent examinations as well as surgical pathology.

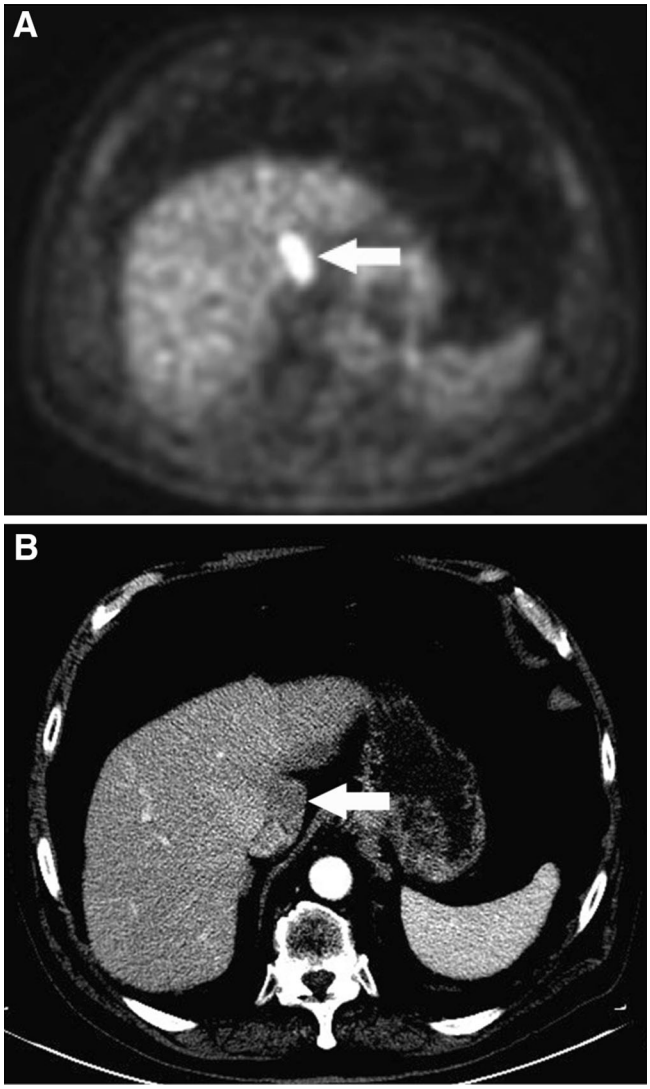

Fig. 1. **A** Axial PET image in a 63-year-old man 5 weeks after completion of neoadjuvant chemoradiation for distal esophageal cancer shows a focus of increased FDG avidity (*arrow*; SUV_{max} 6.0) in the caudate lobe. **B** Corresponding axial contrast-enhanced CT image demonstrates a subtle focus (*arrow*) of reduced enhancement with straight margins. This abnormality resolved on subsequent contrast-enhanced CT (not shown), and the final diagnosis was radiation-induced liver disease.

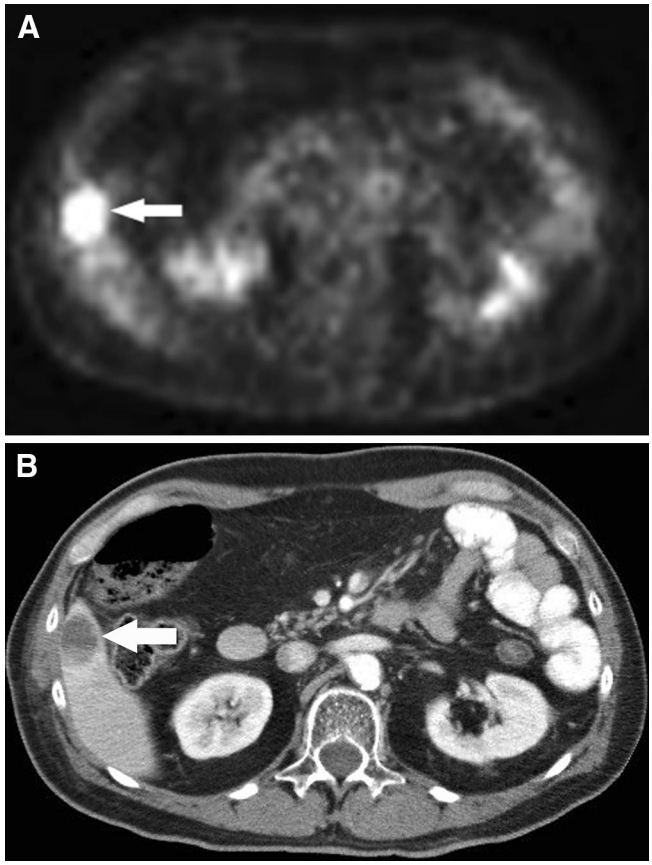

Fig. 2. **A** Axial PET image in a 54-year-old man 5 months after completion of neoadjuvant chemoradiation for distal esophageal cancer shows a focus of increased FDG avidity (*arrow*; SUV_{max} 12.8) in the inferior right lobe. **B** Corresponding axial contrast-enhanced CT image demonstrates a necrotic mass (*arrow*), consistent with a metastasis.

Results

None of the 112 patients had foci of increased FDG uptake visible in the liver on baseline PET/CT. New foci of increased hepatic FDG avidity were seen in 10 of the 112 patients (9%) on the post-treatment PET/CT examinations, 6 (6%) of which had corresponding regions of faint hypoattenuation on the corresponding non-contrast CT. Benignity of the FDG-avid foci was confirmed in 9 (8%) of patients with 1 (1%) patient determined to have metastatic disease (Table 1). The mean SUV_{max} of the FDG-avid foci determined to be radiation-induced liver was 5.7 (range 5.0–8.8). A representative case is illustrated in Figure 1. The patient with confirmed hepatic metastasis (Fig. 2) exhibited a lesion SUV_{max} of 12.8.

Discussion

Common sites of metastatic spread in esophageal cancer include the abdominal lymph nodes, liver, and lungs [10, 23–26]. In one study, it was shown that up to 35 % of patients with esophageal cancer will develop liver metastases [29]. In addition to metastatic disease, the liver is also particularly prone to radiation-induced liver disease during radiotherapy of distal esophageal cancer, due to the close proximity of the left lobe which is accordingly included in the standard radiation field [27–29]. Given that serial PET/CT is increasingly performed during neoadjuvant chemoradiation of esophageal cancer and that both metastases and radiation-induced liver disease may manifest as increased foci of FDG avidity at PET scanning, our study provides important results that address how these two entities might be distinguished.

First, we found that new foci of hepatic FDG avidity developing during neoadjuvant chemoradiation of esophageal cancer are usually due to radiation-induced liver disease. Increased FDG avidity in radiation-induced liver disease results from inflammation caused by radiation with increased FDG uptake by active leukocytes [30]. This simple observational result is statistically reassuring, and likely reflects the low likelihood of metastases developing during neoadjuvant chemoradiation. Second, while based on small numbers, we found that the location of the new foci of FDG avidity may be important. All the foci due to radiation-induced liver disease developed in the left and caudate lobes (Fig. 1), within the presumed radiation field, while the sole case of metastatic disease developed in the inferior right hepatic lobe, remote from the primary tumor and radiation field (Fig. 2).

In a broader context, our study expands the existing literature on ''pseudoprogression'', that is, the development of new findings in cancer patients may falsely indicate disease progression. A study similar to ours evaluating new FDG-avid osseous lesions in patients treated with radiation for pelvic malignancy demonstrated that the lesions were more likely to be insufficiency fractures from osteoradionecrosis than actual disease progression [31]. Perhaps the best known examples of pseudoprogression are increasing blastic change of bone lesions in breast and prostate cancer patients that might suggest worsening of metastases but may actually reflect healing by sclerosis [32, 33]. Other examples include benign sequelae of chemoradiation and surgery that can result in FDG avidity, such as pneumonitis, esophagitis, and osteonecrosis [34]. Diffuse increase in FDG avidity in the bone marrow and spleen is commonly seen after treatment with granulocyte colony stimulating factor, which can also mimic metastases [35].

Our study has several limitations. It was a single institutional retrospective study, with the associated potentials for bias. Our study had some sources of heterogeneity that might be potentially confounding. For example, many of the PET/CT scans were performed at outside institutions and many patients underwent chemoradiation at outside institutions. The details of these PET/CT scans and radiation technique were unavailable to us. Our reference standard was not histological, in most cases. However, the evolution and appearance of the cases of radiation hepatitis and metastatic disease seem sufficiently distinctive that we doubt that misdiagnosis is a significant source of study error.

In conclusion, new foci of increased FDG avidity are commonly seen in the caudate and left hepatic lobes of the liver during neoadjuvant chemoradiation of distal esophageal cancer, and these findings generally reflect radiation-induced liver disease rather than metastatic disease.

Acknowledgments. RAD supported by NIBIB grant 1R25EB016671.

References

1. Alteri R, Anderson K, Barnes C, et al. (2013). Estimated number of new cancer cases and deaths by sex, US, 2013. American Cancer Society: Cancer Facts and Figures 2013. http://www.cancer.org/research/cancerfactsstatistics/cancerfactsfigures2013/. Accessed 21 Oct 2013
2. Bosch DJ, Muijs CT, Mul VE, et al. (2014) Impact of Neoadjuvant Chemoradiotherapy on Postoperative Course after Curative-Intent Transthoracic Esophagectomy in Esophageal Cancer Patients. Ann Surg Oncol 21(2):605–611
3. Van Hagen P, Hulshof MCCM, van Lanschot JJB, et al. (2012) Preoperative chemoradiotherapy for esophageal or junctional cancer. N Engl J Med 366:2074–2084
4. Urschel JD, Vasan H (2003) A meta-analysis of randomized controlled trials that compared neoadjuvant chemoradiation and surgery versus surgery alone for resectable esophageal cancer. Am J Surg 185:538–543
5. Bosset J, Gignoux M, Triboulet J, et al. (1997) Chemoradiotherapy followed by surgery alone in squamous cell carcinoma of the esophagus. N Engl J Med 337:161–167
6. Bates BA, Detterbeck FC, Bernard SA, et al. (1996) Concurrent radiation therapy and chemotherapy followed by esophagectomy for localized esophageal carcinoma. J Clin Oncol 14:156–163
7. Donington JS, Miller DL, Allen MS, et al. (2003) Tumor response to induction chemoradiation: influence on survival after esophagectomy. Eur J Cardiothorac Surg 4:631–637
8. Swisher SG, Ajani JA, Komaki R, et al. (2003) Long-term outcome of phase II trial evaluating chemotherapy, chemoradiotherapy, and surgery for locoregionally advanced esophageal cancer. Int J Radiat Oncol Biol Phys 1:120–127
9. Kim TJ, Kim HY, Lee KW, Kim MS (2009) Multimodality assessment of esophageal cancer: preoperative staging and monitoring of response to therapy. Radiographics 29:403–421
10. Daly JM, Fry WA, Little AG, et al. (2000) Esophageal cancer: results of an American College of Surgeons Patient Care Evaluation Study. J Am Coll Surg 190:562–572
11. Bruzzi JF, Munen RF, Truong MT, et al. (2007) PET/CT of esophageal cancer: its role in clinical management. Radiographics 27:1635–1652
12. Levine EA, Farmer MR, Clark P, et al. (2006) Predictive value of 18-fluoro-deoxy-glucose-positron emission tomography (18F-FDG PET) in the identification of responders to chemoradiation therapy for the treatment of locally advanced esophageal cancer. Ann Surg 243:472–478
13. Iyer RB, Balachandran A, Bruzzi JF, et al. (2007) PET/CT and hepatic radiation injury in esophageal cancer patients. Cancer Imaging 7:189–194
14. Itai Y, Murata S, Kurosaki Y, et al. (1995) Straight border sign of the liver: spectrum of CT appearances and causes. Radiographics 15:1089–1102
15. Unger EC, Lee JKT, Weyman PJ (1987) CT and MR Imaging of Radiation Hepatitis. J Comput Assist Tomogr 11:264–268
16. Kawamoto S, Soyer P, Fishman EK (1998) Nonneoplastic liver disease: evaluation with CT and MR imaging. Radiographics 18:827–848
17. Lee JKT, Sagel SS, Stanley RJ, et al. Computed Tomography with MRI Correlation.
18. Willmart S, Nicaise N, Struyven J, et al. (2000) Acute radiation-induced hepatic injury: evaluation by triphasic contrast enhanced helical CT. Br J Radiol 73:544–546
19. Suto YS, Kato T, Yoshida K (1996) MRI Findings in Radiation-Induced Hepatic Injuries. Yonago Acta Medica 39:127–134
20. Yankelevitz DF, Knappp PH, Henschke Cl (1992) MR appearance of radiation hepatitis. Clin Imaging 16:89–92
21. Gazelle GS, Saini S, Mueller PR (1997) Hepatobiliary and Pancreatic Radiology: Imaging and Intervention. New York: Thieme Medical Publishers, Inc.; pp. 289.
22. Eisenberg RL (1996) *Gastrointestinal radiology: a pattern approach*. Hagerstown: Lippincott-Raven Publishers, p 1118

23. Bruzzi JF, Swisher SG, Truong MT, et al. (2007) Detection of interval distant metastases: clinical utility of integrated CT-PET imaging in patients with esophageal carcinoma after neoadjuvant therapy. Cancer 109:125–134
24. Quint LE, Hepburn LM, Francis IR, et al. (1995) Incidence and distribution of distant metastases from newly diagnosed esophageal carcinoma. Cancer 76:1120–1125
25. Mandard AM, Chasle J, Manray J, et al. (1981) Autopsy findings in 111 cases of esophageal cancer. Cancer 48:329–335
26. Feldman M, Friedman LS, Brandt LJ (2010) *Sleisenger & Fordtran's gastrointestinal and liver disease*, 9th edn. Philadelphia: Saunders, pp 745–767
27. Domachevsky L, Jacene HA, Sakellis CG, Kim CK. Postradiation Changes in Tissues: Evaluation by Imaging Studies with Emphasis on Fluorodeoxyglucose-PET/Computed Tomography and Correlation with Histopathologic Findings. PET Clinics. DOI: 10.1016/j.cpet.2013.10.005. Review article (In Press Corrected Proof) 12 December 2013
28. Wong JJ, Anthony M-P, Khong PL (2012) Hepatic radiation injury in distal esophageal carcinoma: a case report. Clin Nucl Med 37:709–711
29. Nakahara T, Takagi Y, Takemasa K, et al. (2008) Dose-related fluorodeoxyglucose uptake in acute radiation-induced hepatitis. Eur J Gastroenterol Hepatol 20:1040–1044
30. DeLappe EM, Truong MT, et al. (2009) Hepatic radiation injury mimicking a metastasis on positron-emission tomography/computed tomography in a patient with esophageal carcinoma: a case report. J Thorac Oncol 37(7):709–711
31. Coakley FV, Saltavi A, Costouros NG, et al. (2011) F-18 FDG PET/CT findings in postradiation pelvic insufficiency fracture. Clin Imaging 35:139–142
32. Pollen JJ, Shlaer WJ (1979) Osteoblastic response to successful treatment of metastatic cancer of the prostate. Am J Roentgenol 132:927–931
33. Janicek MJ, Hayes DF, Kaplan WD (1994) Healing flare in skeletal metastases from breast cancer. Radiology 192:201–204
34. Ulaner GA, Lyall AL (2013) Identifying and distinguishing treatment effects and complications from malignancy at FDG PET/CT. Radiographics 33:1817–1834
35. Mettler FA, Guiberteau MJ (2012) *Essentials of Nuclear Medicine*, 6th edn. Philadelphia: Elsevier Saunders, pp 373–374